From Zachary H. Taxin, Samuel A. Neymotin, Ashutosh Mohan,Peter Lipton, William W. Lytton, Modeling Molecular Pathways of Neuronal Ischemia. In Kim T. Blackwell, editor: *Progress in Molecular Biology and Translational Science*, Vol. 123, Burlington: Academic Press, 2014, pp. 249-275.
ISBN: 978-0-12-397897-4

Academic Press
Elsevier

CHAPTER ELEVEN

Modeling Molecular Pathways of Neuronal Ischemia

Zachary H. Taxin*, Samuel A. Neymotin*, Ashutosh Mohan*, Peter Lipton†, William W. Lytton*

*Department of Physiology & Pharmacology, SUNY Downstate, New York, USA
†Department of Neuroscience, University of Wisconsin, Madison, Wisconsin, USA

Contents

1. Critical Initiator Events in Ischemic Pathways 251
2. Models of Molecular Pathways in Ischemia 253
   - 2.1 Model of ionic dysregulation and cytotoxic edema 254
   - 2.2 Model of astrocytic protection 256
   - 2.3 Model of Ca^{++} dynamics and mitochondrial permeability 257
   - 2.4 Model of death by ROS 259
   - 2.5 Nitric oxide as a broadcast signal 259
   - 2.6 BN model of apoptotic protein regulation 260
   - 2.7 BN model of ROS effects and gene regulation 263
   - 2.8 Kinetic model with Boolean macroparameters for gating of apoptosis signals 264
   - 2.9 Two-dimensional model of damage and stress response 267
   - 2.10 Analyzing cell fate decisions with an ODE-based regulatory gene network model 268
   - 2.11 Modeling evolution of the penumbra 269
3. Pitfalls and Outlook 272

References 274

Abstract

Neuronal ischemia, the consequence of a stroke (cerebrovascular accident), is a condition of reduced delivery of nutrients to brain neurons. The brain consumes more energy per gram of tissue than any other organ, making continuous blood flow critical. Loss of nutrients, most critically glucose and O_2, triggers a large number of interacting molecular pathways in neurons and astrocytes. The dynamics of these pathways take place over multiple temporal scales and occur in multiple interacting cytosolic and organelle compartments: in mitochondria, endoplasmic reticulum, and nucleus. The complexity of these relationships suggests the use of computer simulation to understand the

Progress in Molecular Biology and Translational Science, Volume 123
ISSN 1877-1173
http://dx.doi.org/10.1016/B978-0-12-397897-4.00014-0

interplay between pathways leading to reversible or irreversible damage, the forms of damage, and interventions that could reduce damage at different stages of stroke. We describe a number of models and simulation methods that can be used to further our understanding of ischemia.

Neuronal ischemia is a condition of transient or chronic low blood flow to the brain. Stroke (also called cerebrovascular accident, CVA) is a consequence of ischemia. In the United States, stroke is the fourth leading cause of death and is a major cause of disability and functional cognitive impairment, particularly in aging populations.[1]

The brain consumes more energy per gram of tissue than any other organ. Hence, ample cerebral blood flow and its autoregulation are critical to neuronal functioning. Loss of blood flow for even a few minutes triggers irreversible damage, only partially offset by neuroprotective mechanisms. Recently, much research has focused on elucidating these mechanisms for control of intrinsic neuroprotective pathways in order to help design therapeutic interventions. The complexity of the many different cellular and subcellular signaling pathways involved makes computer modeling an important tool for studying ischemia.

A stroke can be subdivided into a central area of severe ischemia, the ischemic core, and a surrounding area of damaged tissue, the ischemic penumbra. This penumbral area is considered the best target for recovery, as its cells still retain some viability. Therefore, in discussing the patterns of damage at the cellular and molecular level, we must explore the consequences of ischemia in both areas, considering also the damaging effects of cell death at the core through influence on the penumbra via local diffusion of released toxic cell contents.

Several of the models to be presented discuss the effects of *preconditioning*. Preconditioning is a therapeutic approach in which a pretreatment is used in order to prepare the brain for subsequent stroke, by initiating the varieties of intrinsic neuroprotective proteins and pathways. The most obvious preconditioning paradigm uses prior mild ischemia to trigger these changes, thereby providing partial protection against the effects of the more major subsequent event. However, this is not an approach that can be used clinically, due to the difficulty of titrating an appropriately minor ischemia, to avoid triggering the irreversible processes that would themselves produce an immediate stroke. Other preconditioning techniques utilize pharmacotherapeutic methods to activate these pathways.

1. CRITICAL INITIATOR EVENTS IN ISCHEMIC PATHWAYS

Ischemia triggers dysfunction in several pathways, with multiple final outcomes which include multiple paths to death or to recovery. The pathways to death include (1) apoptosis: programmed cell death which permits cells to fold inward in a controlled manner; (2) necrosis: uncontrolled cell collapse with membrane disruption releasing multiple toxic cell contents; (3) necroptosis: an intermediate condition where apoptosis is begun but cannot complete due to further disruption. Although the endgames differ, all ischemic events start with a similar set of initial cellular events that progress in a characteristic sequence, triggered after a 1- to 3-min period of metabolite reduction. However, following this initial sequence, ischemia sets in motion an extremely diverse set of enzymatic, control-cascade, mechanical, proteomic, and genomic changes that occur across many temporal scales, and which interact across milliseconds to days in various combinations. Some ischemic insults will cause immediate cell death via cytotoxicity and necrosis, whereas other levels of insult engage programmed cell death over several days. Still others will leave cells in various stages of prolonged attempted recovery. These many pathways suggest the possibility of many different points of possible therapeutic intervention at different temporal stages and in different parts of the umbra/penumbra.

All cells require glucose and O_2 to run oxidative phosphorylation in the mitochondria for production of adenosine triphosphate (ATP), the major energy currency within cells. Without these metabolites, cellular respiration will cease, rapidly diminishing available ATP. For this reason, some cell types maintain alternative short-term energy stores, allowing compensation for transient reductions in oxygen delivery to tissue. In particular, muscle and liver maintain significant stores of glycogen which serve to keep glucose levels from falling during exercise when metabolite levels are reduced. Creatine phosphate is another store of energy, good for up to 5 s of cellular activity. Unlike other tissues in the body, neurons and glia do not have a substantial energy reservoir. Glycogen is found in small amounts in glia, but is almost absent in neurons. Creatine phosphate exists in most brain tissue cells, but only provides brief respite from metabolic lack. Therefore, within 1–2 min of oxygen and glucose deprivation that occurs in complete ischemia, ATP levels in brain tissue fall to roughly 20% of their control levels.

Among the myriad homeostatic roles of ATP is the energy for the Na^+/K^+-ATPase pump that maintains the transmembrane ionic gradients for these two major ions, thereby maintaining resting membrane potential. In neurons, this pump must be tightly regulated to ensure appropriate conditions for firing action potentials. When the Na^+/K^+-ATPase fails, intracellular Na^+ increases dramatically. Functional consequences of this shift in equilibrium include: loss of signaling control, changes in cell volume, and swelling of cell organelles. Ionic dysregulation also causes anoxic membrane depolarizations, whereby large number of cells begin to depolarize significantly over long periods of time. These depolarizations cause further damage.

Loss of O_2 and reduced cellular respiration also results in the formation of reactive oxygen species (ROS), which are devastating to the cell. ROS are highly reactive species which damage both proteins and nucleic acids. ROS are generated during normal oxidative phosphorylation. But, in the healthy cell, ROS are then passed on to a set of conversion methods which transform them into water-soluble species that can be readily eliminated by the cell. As the mitochondrial machinery for respiration is interrupted, the cell begins to accumulate these intermediate ROS. Additional ROS are produced by generation of free fatty acids from mitochondrial membranes due to upregulation of oxygenase proteins (e.g., cyclo-oxygenase-2 or lipoxygenase). In addition to further damaging transmembrane pumps and other homeostatic control proteins, ROS are particularly damaging to DNA. Damage to DNA is a key initiating factor in control of the p53 protein, which is directly responsible for cell fate commitment leading to cell death via apoptosis. ROS production is particularly important in the penumbra and can increase markedly after reperfusion, reducing the efficacy of treatments that restore blood flow.

As respiration fails, increased intracellular Na^+ and consequent depolarization leads to glutamate being released into surrounding tissue. Extracellular glutamate, as an excitatory neurotransmitter, then opens synaptic channels causing influx of Ca^{++}, Na^+, and K^+, and further contributing to intracellular ion dysregulation, a phenomenon known as excitotoxicity. Ca^{++} is a major second messenger used in many pathways. A pathological increase in Ca^{++} is particularly deleterious, leading to further loss of homeostasis and disruption of multiple Ca^{++}-dependent pathways. Increased Ca^{++} levels also serve as a signal to initiate cell death pathways,[2] such that inhibitors of calpain (a Ca^{++}-activated protease) can markedly reduce cell death in *in vivo* animal models.[3] Ca^{++} rise is further augmented

by release from intracellular stores in endoplasmic reticulum (ER) and mitochondia through Ca^{++}-induced Ca^{++} release (CICR), as well as due to reversal of membrane Na^{+}–Ca^{++} ion exchange pumps.[4] In addition to its role in regulating cellular subprocesses (e.g., calmodulin, calbindin, CaMKII, etc.,), Ca^{++} is involved in mitochondrial and nuclear regulation. Although it remains somewhat unclear to what extent normal Ca^{++} regulatory processes are localized to these separate organelles, it is clear that Ca^{++} does pass readily across compartments, for example, being taken up by mitochondria from the surrounding cytosol.

In summary, the loss of ATP during ischemic insult is the prime mover for a series of interrelated signaling cascades with multiple important consequences that include:

- Ionic homeostasis dysregulation depolarizing resting membrane potential
- Generation of ROS, damaging proteins, DNA, and membranes
- Release of glutamate leading to excitotoxicity
- Increased intracellular Ca^{++}
- Loss of cell volume control
- Mitochondrial instability due to volume changes and ion flux

With the cell destabilized in these many ways, it may follow one of several paths that lead to cell death. Alternatively, following vascular reperfusion, the cell may return to a near-normal state. It is crucial to note that some changes are transient and reversible, while others represent major alterations in homeostatic cell processes that have inevitable negative consequences.

2. MODELS OF MOLECULAR PATHWAYS IN ISCHEMIA

There are several approaches used to model molecular pathways: stochastic modeling techniques at various levels of granularity, detailed mass-action kinetic models using systems of ordinary differential equations (ODEs), and reaction-scheme methods such as the Boolean network (BN) formalism.

This ordering of methods reflects decreasing modeling precision. The most detailed stochastic models, those that follow individual molecules using a Monte Carlo method,[5] require the most detailed parameterization, requiring the availability of large amounts of experimental detail, which may not always be available. Additionally, such models require substantial computer resources, making them impractical for very large problems such as a simulation of an entire neuron. At the other extreme, a BN provides only a very

gross approximation of the underlying reality, capturing a sequence of molecules which turn other molecules on or off with no indication of rate or of other complexities of bimolecular reactions. Such schemes have the advantages of requiring only limited experimental data and running quickly as simulations. An additional aspect of molecular modeling is the movement of molecules by diffusion (reaction–diffusion techniques) or by transport across subcellular compartments and organelles.

Several models, using a variety of techniques, have been developed to assess molecular pathways in ischemic injury. We discuss several of them here.

2.1. Model of ionic dysregulation and cytotoxic edema

In the models of Dronne *et al.*[4,6], the key components of an evolving stroke can be grouped into 10 interacting submodels: (1) Metabolic reactions within the cell (O_2 lack, loss of ATP); (2) ionic dysregulation; (3) development of cytotoxic edema due to ionic disturbances and excitotoxic changes; (4) glutamate-dependent excitotoxicity; (5) spreading waves of glutamate depression; (6) nitric oxide (NO) synthesis; (7) tissue inflammation and local inflammatory response; (8) necrosis; (9) apoptosis; and (10) reperfusion-dependent tissue changes. Although the models interact, they can be evaluated independently as well.

We will focus here on one of their models,[4] a model of the development of cytotoxic edema—water accumulation within cells. Edema is caused by water following ion fluxes, and is one way that large-scale, tissue-wide changes can be linked to disturbances at the molecular scale. In addition to cytotoxic edema, stroke will cause other forms of edema, vasogenic and mechanical, that will also have profound effects.

In the Dronne model, intraneuronal space, intra-astrocytic space, and extracellular space were modeled as separate compartments. For simplification, it was assumed that the system was closed and that global volume remained constant. Five main species Na^+, K^+, Ca^{++}, Cl^-, and glutamate were considered in the model.

In this model, compartment volumes, represented as a fraction of a constant total volume, altered with species flux as water followed ionic gradients to maintain osmotic equilibrium. Volume changes were the consequence of time-dependent variations in species concentrations due to passage across membranes, modeled as occurring through the many voltage-gated channels, volume-activated channels, pumps, exchangers, and ligand-gated channels. However, open probabilities for channels were defined at steady

state rather than using dynamic gating, because only consequences of long-term ischemic insult were being studied. Neuron and astrocyte compartments reached osmotic equilibrium following ionic disturbance. The volume of extracellular space was then calculated based on total volume. This is a clinically relevant measure because the ratio of the apparent diffusion coefficient of water can be measured using diffusion-weighted MRI scan, and is used as an indicator of the severity of acute stroke.[7]

A related change in the cellular microenvironment immediately after ischemic onset is a rise in extracellular K^+ due to activation of voltage- and Ca^{++}-dependent K^+ channels with depolarization as well as failure of the Na^+–K^+ pump. The other species which accumulated in the extracellular space was glutamate, released due to depolarizing potentials that triggered synaptic release, as well as failure of the glutamate carrier to uptake and remove glutamate from the extracellular space. Intracellularly, Ca^{++} increases of nearly 4 orders of magnitude were observed in the neuron compartment. These intracellular Ca^{++} dynamics were shown to be relatively slow, reaching their maxima nearly twice as slowly as changes in other ion concentrations. This slow dynamics was attributed to the Ca^{++} changes being primarily due to reversal of Na^+–Ca^{++} exchange leading to Ca^{++} influx. The process of Ca^{++}accumulation was increased further by NMDA receptor activation by extracellular glutamate, as well as Ca^{++}-induced Ca^{++} release from within the cell.

Having explored the natural history of ischemia in the model, the authors then looked at manipulation of individual channel conductances, in order to determine where modulation of channel activations might have protective effects in terms of reduction in edema. An increase in persistent Na^+ channel density was found to have a deleterious effect, promoting cytotoxic edema, suggesting that pharmacological blockade of this channel might be protective. By contrast, *increasing* conductance of the delayed rectifier K^+ channel was protective.

The model suggested the hypothesis of a causal sequence for development of edema, leading from pump failure to depolarization to pathological voltage- and Ca^{++}-dependent channel activation. These failures are then propagated by ionic imbalances across membranes compartments. Ion dysfunction cannot be fully compensated by non-ATP-based transmembrane ion exchangers or leak channels, which have little ability to stabilize fluxes after failure of energy-driven pumps.

As with all models, it is important to consider the results in the context of what the modelers left out. The model is primarily at the multicellular and

tissue scale spatially and at the minutes-to-hours temporal scale. It therefore ignores neuronal network effects as well as more detailed intracellular molecular effects. Regional distribution of neurons and glia is not homogeneous throughout the brain, so the model might need to be modified to consider effects of ischemia in different brain areas. Of necessity, some types of channels and ions were omitted—in particular effects of pH and pCO_2, though acidity can have a large effect on cytotoxicity. The parameters used were optimized from a variety of sources to produce a steady state for the model. Not only were transient dynamics thereby omitted, but the approach also raises concerns as to whether typical steady-state values would still hold in the context of ischemic tissue, due to alterations in intrinsic ion-channel modulation by second messengers and phosphorylation state.

2.2. Model of astrocytic protection

Diekman *et al.* recently developed a model that explores how IP_3-mediated Ca^{++} release in astrocytes may protect against their involvement in cytotoxic edema and other local microenvironment damage.[8] This astrocyte model built on the classic ER CICR model of Magnus and Keizer.[9] The model looked at state variables for Ca^{++}, ATP, ADP, pH, NADH in the cytosolic, ER, and mitochondrial compartments. As in the prior model, ischemia caused the astrocytes to lose the ability to maintain electrochemical gradients due to loss of energy sources.

Ischemia was simulated by reducing glucose and O_2 inputs by a constant percentage at a given time. The two metabolites were tested individually and together: similar results were found with these three interventions—increased cell volume, depolarized membrane, and reductions in ATP, NADH, and Ca^{++}. Next, with both metabolites reduced jointly, IP_3 production was augmented, as can be done pharmacologically using an astrocyte-specific receptor. With a short period of ischemia, addition of IP_3 caused mitochondrial Ca^{++} to return to a higher level, improving ATP production. In another set of simulations, a mitochondrial K_{ATP} channel was included and also had a protective effect. These results suggested that loss of mitochondrial Ca^{++} homeostasis might be destabilizing, such that restoration of Ca^{++} levels could prevent an unfavorable outcome.

This work demonstrated a mechanism by which regulation of astrocyte Ca^{++} metabolism could have significant neuroprotective effects against loss of energy substrates in ischemia. However these protective mechanisms,

stimulation of IP_3 and the K_{ATP}, would only work up to a certain point. Beyond that point Ca^{++} is too severely destabilized for recovery to occur. The model also suggested that metabolically impaired astrocytes could use high Ca^{++} to signal distress to downstream effectors of cell death.

2.3. Model of Ca^{++} dynamics and mitochondrial permeability

Alterations in mitochondrial permeability appear to be a common pathway leading to cell death in a number of pathological conditions, including ischemia. Experimental research has led to the identification of a permeability transition pore (PTP) as a cause of a pathological mitochondrial permeability transition which is related to increased intracellular Ca^{++}. Oster *et al.* explored a model of how intracellular Ca^{++} dynamics would produce changes in mitochondrial membranes which would lead to cell death.[10] This model was also built by extending the Magnus–Keizer model of CICR.[11]

Mitochondria use an electrochemical proton gradient to run the ATPase pump during oxidative phosphorylation, thereby generating ATP. This process has the secondary effect of sequestering free cytosolic Ca^{++} via a uniporter mechanism driven by the proton-based mitochondrial electrical gradient. ATP-dependent Ca^{++} pumps and Ca^{++}–Na^{+} exchange also play a role and are also included in the model. The model added dynamic pH buffering by inorganic phosphates and a pH-dependent activation mechanism for the PTP to the basic model of CICR. Further channel dynamics were included, allowing for Ca^{++} uptake saturation.

The PTP was itself modeled as a three-state channel: closed, open low-conductance (PTP_l), and open high-conductance (PTP_h). Transitions from PTP_l to PTP_h required elevated mitochondrial Ca^{++} levels. Once the PTP_h state was achieved, it remained constitutively open. This led to cell death via extrusion of mitochondrial proteins such as Cytochrome C. Cytochrome C catalyzed feedforward activation of procaspases, the intrinsic cytosolic enzymes involved in the apoptosis pathway. The activation of the PTP_h state can therefore be considered an irreversible step towards cell death.

Changes in PTP_l state were modeled as dependent upon proton concentration in the mitochondria (H_M), where the opening rate and time constant of activation (τ_l) were also both dependent upon proton concentration using a variation on the Hodgkin–Huxley parameterization via steady state and time constants which are here dependent on H_M, and parameterized with amp_τ, and p_i:

$$\frac{\mathrm{dPTP_l}}{\mathrm{d}t} = \frac{[\mathrm{PTP_{l\infty}}(H_\mathrm{M}) - \mathrm{PTP_l}]}{\tau_\mathrm{l}(H_\mathrm{M})}$$

$$\mathrm{PTP_{l\infty}}(H_\mathrm{M}) = 0.5 \cdot \left(1 + \tan h\left(\frac{p_1 - H_\mathrm{M}}{p_2}\right)\right)$$

$$\tau_\mathrm{l}(H_\mathrm{M}) = \frac{\mathrm{amp}_\tau}{\cos h\left(\frac{H_\mathrm{M} - p_3}{p_4}\right)} + p6$$

Ca^{++} flux through the PTP was assumed to be similar to flux through the uniporter.

Experiments have demonstrated that the cell's transition to an unhealthy state may require an extended period of time for full development, depending on the severity of damage. Therefore, modules were added to quantify PTP state transitions over long-term Ca^{++} fluctuations in the cell. This part of the model included a time-delay function in the equation for change in the PTP_h gate state. Similarly, a threshold equation was developed that took into account time-dependent Ca^{++} concentration changes within the mitochondria. Further equations modeled proton flux and proton buffering. Because these dynamics are poorly understood within mitochondria, a simple sigmoidal functional of acid buffering based on proton concentration within the mitochondria was used. Ca^{++} diffusion was modeled within the cytoplasm with no explicit cytoplasmic buffering. However, an effective diffusion constant (K_{eff}) was used based on the modification expected due to a fixed concentration of buffer (B_T) and a single dissociation constant (K_C): $D_{\mathrm{eff}} = D_{\mathrm{ca}} \cdot K_\mathrm{C}/(B_\mathrm{T} + K_\mathrm{C})$.

Simulations were performed by inducing pulses of Ca^{++} at varying intensities over varying time scales. This was intended to mimic aspects of oscillating Ca^{++} pulse waves that occur as a result of the CICR and increased cytosolic Ca^{++} that would result from an ischemic insult. While slow pulses (three pulses of 2 s each over 90 s interval) could be adequately buffered by the mitochondria, fast pulses (three pulses of 2 s each over 25 s) resulted in transient mitochondrial depolarizations that caused release of sequestered Ca^{++} into the cytoplasm. Slow and fast pulses also differed in how they affected mitochondrial pH. Slow pulses caused transient pH elevations that were compensated, whereas rapid pulses caused pH to exceed threshold levels for a long enough time that the PTP_l state was activated. Overall, Ca^{++} recovery via sequestration was found to occur faster than pH buffering.

2.4. Model of death by ROS

The generation of ROS is a powerful stimulus for cell death via damage to mitochondria and DNA. Low concentrations of ROS are produced during normal respiration. The cell eliminates these with scavenging enzymes and uncoupling proteins. As their names suggest, scavenger proteins search and absorb toxic species, while uncouplers physically disconnect elements of the electron transport chain to reduce ROS production. Excess ROS, exceeding the capacity of scavenging, is produced in the mitochondria when the electron transport chain fails.

The major electron donors to the oxidative chain are NADH and $FADH_2$, which are reduced through passage of the high-energy electron through the cytochromes. Heuett and Periwal developed a cell-scale model for production and regulation of ROS in response to metabolic dysfunction based on changes in NADH and $FADH_2$ concentration.[12] These were modeled as a function of glucose and oxygen availability. ATP concentration was also included and was dependent upon tricarboxylic acid cycle flux, F1–FO ATPase flux, and the efflux of ATP removal from the mitochondrium. The instantaneous rate of change for ROS concentration was given by the sum of its generation fluxes (from NADH and $FADH_2$) and its removal fluxes by scavenger and uncoupling proteins. Initial conditions included the concentration of NAD and FAD. Further modifications to the model took into account ROS-induced suspension of electron transport, and change in proton leak across the membrane. This allowed a way to test several mechanisms of pH change and Ca^{++} flux due to cellular damage.

2.5. Nitric oxide as a broadcast signal

Alam *et al.* explored the relationship between Ca^{++} concentrations and the feedback oscillation of apoptotic control proteins in the context of cellular stress.[13] Although cell stress can occur in a variety of ways, the most common is oxidative stress due to metabolic dysfunction. Once again, Ca^{++} is implicated, here increasing production of nitric oxide (NO) via its synthases. NO is a regulator of subcellular processes, and induction of NO has been demonstrated to be significant in the apoptotic decision.[14] A major downstream target of NO is Mdm2, which is a negative regulator of p53. p53 is a proapoptotic control protein and a primary regulator of cell fate decisions and changes in cell cycle activity. NO disrupts the inhibitory effect of Mdm2 by forming an Mdm2–NO complex that eliminates Mdm2 effects on p53. Mdm2 and p53 both have short half-lives, approximately

15–30 min. Therefore, levels of these proteins are constantly shifting, along with their transcription regulation. NO, a gas, diffuses extremely rapidly and can move directly through membrane, allowing it to have a volume effect.

Various levels of Ca^{++} concentration were tested for their effect on the oscillation dynamics of Mdm2 and p53. Levels of stability were identified which depended on the rate of Ca^{++} production: (1) a stable regime where Mdm2–p53 oscillation yielded apoptosis, (2) a partly stabilized regime with a damped oscillation. The effects of Ca^{++} oscillations were also tested. The results suggested that oscillating waves of diffusible Ca^{++} could induce widespread changes in p53 activity across the cell, and that independent Mdm2–p53 systems in different regions could be simultaneously activated by a sufficient Ca^{++} stimulus. The consequences of stochastic variation were then explored. High noise disrupted oscillations. With reduced noice, the multiple systems become synchronized, causing p53 oscillations to generate apoptosis. Stochastic noise could partially mask the effects of Ca^{++} on the Mdm2–p53 population when the system size was small. As the system increased, further coordination pushed the cell towards signal synchronization.

Taken together, these results showed how Ca^{++} levels could act as signal integrators for the downstream regulation of networks of cell cycle proteins. Such signaling would be highly dynamic and would involves feedback fluctuations and oscillations. An important stochastic element was suggested for the network regulation of apoptosis, with the level of noise directly correlated to system stability.

2.6. BN model of apoptotic protein regulation

In assessing complex system behavior, it can be helpful to distil the multifactorial elements such that stability and characteristics of the system under different conditions can be more readily modeled. The BN formalism provides a convenient way to model apoptotic pathways by using binary rules for pathway relationships.

The model of Mai *et al.* used BNs to explore the apoptosis network.[15] Both intrinsic and extrinsic pathways were represented: 40 nodes represented both extracellular mediators (TNF, tumor necrosis factor, which is proapoptotic; GF, growth factor—protective) and intracellular mediators (TRADD, Caspases, Akt, NFkB, p53, etc.,). The intrinsic pathway also included mitochondrial proteins in the Bcl-2 and Bax families. To simplify the model, some molecules with similar functions were combined in a single

node. The model was divided into functional groups; pathways were generally grouped as being proapoptotic or prosurvival, although it was the behavior of the system with particular initial conditions and extrinsic influences that would determine how they interacted: proteins might have multiple functions depending on coactivations. Connections at p53 were given especial attention because of this protein's critical function as the final common pathway for cell fate. p53 received inputs from extrinsic and intrinsic apoptotic signals, as well as prosurvival signals from the Akt pathway.

The network was driven through activation of the extrinsic pathways which activate transmembrane domains leading to a sequence of feedforward reactions though the caspaces. Nodes are Boolean, either ON or OFF. To determine a node state, activating (A) and inactivating (H) inputs were compared at a given time-step:

$$S_i(t+1) = \left\{ \begin{array}{ll} \text{OFF} & \text{if } A_i(t) < H_i(t) \\ \text{ON} & \text{if } A_i(t) > H_i(t) \\ S_i(t) & \text{if } A_i(t) = H_i(t) \end{array} \right\}$$

Current node state depends only on the inputs at the current iteration except when the S remains unchanged. Note that the network included both feedforward and feedback loops (Fig. 11.1).

At the beginning of each simulation, all internal nodes had an initial probability of 0.5 to be in the OFF or ON state. A network state could then be defined as a particular vector of node states. Each exploration of system fate assessed thousands out of the 2^{40} possible randomized initial network states in the context of particular inputs. This represented the concept that the network would be taken unaware by the sudden onset of a stroke with arrival of the extrinsic apoptotic signals. However, it neglects the likelihood that the network generally exists in some subspace of stable dynamical modes that are favored. Initial networks states that always led to cell death, for all inputs, were omitted from further analysis. After running the randomizations, the possible outputs were evaluated statistically. A *DNA damage event node* that remained turned on for more than five time-steps was considered lethal. If a certain number of time-steps occurred without activating that node that was considered survival. Survival in the context of an input could be defined by a unique set of initial network states. These states could then be tested for stability by perturbing the system by swapping one or two nodes and determining if the system still permitted survival. Network states which were stable for survival were explored in greater depth.

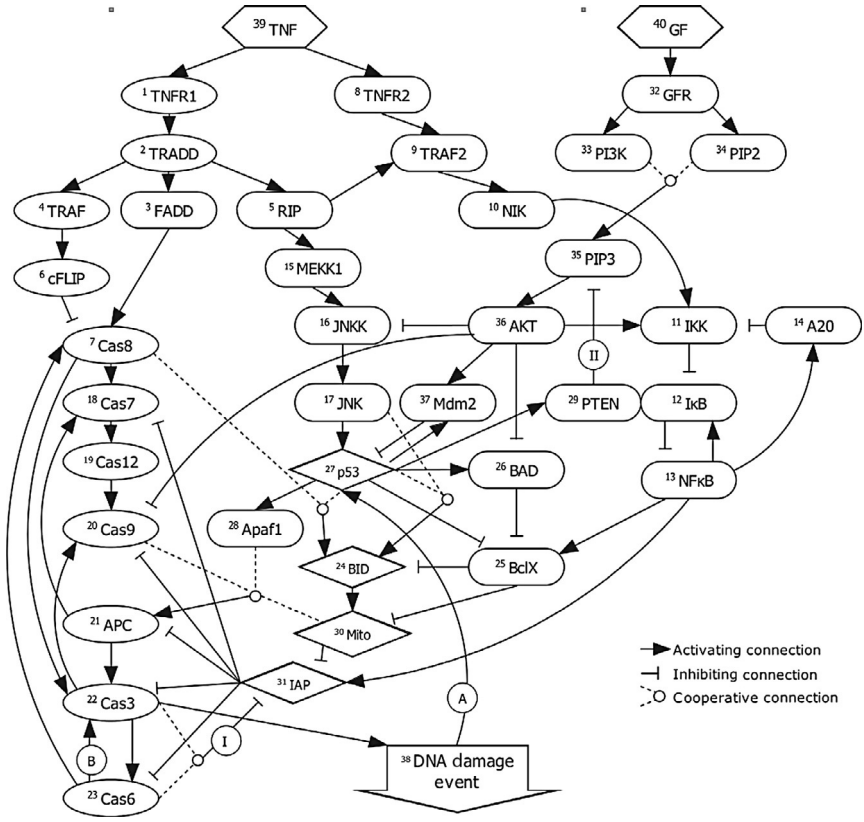

Figure 11.1 Schematic for BN model shows both feedforward and feedback loops from the extrinsic inputs at top to the potential for DNA damage at bottom. Note the sequence of caspaces down the left side which lead to the final *DNA damage event* at the bottom.[15]

Statistical analysis of different sets allowed determination of key nodes in initial states that were lethal in situations where no external apoptotic signals were given, or when protective growth factors were stimulated. These results were compared to damaged models, in which specific connections between internal nodes were severed (edge-ablations), simulating the potential for damage to intermediate signal proteins by ROS. An apoptosis ratio was defined as the number of initial states causing apoptosis divided by the total number of initial states. This ratio was then compared in 16 models with different edge-ablation combinations and across several different input signal combinations. For instance, the apoptosis ratios in a model with pathways blocked was compared for simulations with no external signal

(i.e., steady state), growth factor alone, TNF alone, or both TNF and growth factor signals. These simulations also included signal interruptions for TNF and mitochondrial signals (represented as a single node).

Several conclusions emerged from this work. (1) The intrinsic state values are less important than extrinsic signaling in determining the cell fate. (2) A set of points in state space are identifiable which represent an irreversible pathway to apoptosis. In some cases, this fate could be predicted considerably ahead, indicating that the process could be a prolonged one that might be susceptible to external intervention. (3) Loss of a specific pathway could significantly affect probability of apoptosis. (4) Stability varied among survival network states. Greater concentrations of extrinsic (protective) growth factor increased cell stability. Overall, these results are consistent with experimental evidence, which has demonstrated surprising variability of apoptosis in ischemic preparations. Therapeutically, this approach will allow us to separate mechanisms with different pathways to their fate, with different mechanisms suggesting different approaches to intervention.

2.7. BN model of ROS effects and gene regulation

In the prior model, DNA damage was considered the final event that induces apoptosis. In a recent paper, Sridharan *et al.* (2012), modeling p53-mediated apoptosis in response to ROS-induced DNA damage, used gene regulation to explore mechanisms of ROS cytotoxicity.[21] This model also used the BN approach to localize points of pathway control. The modeling approach used here added the method of *fault identification*. Fault identification is an engineering method used to determine the vulnerability of electronics or other complex systems to failure of a single component.

Cells contain a variety of mechanisms for dealing with generation of ROS. Nrf2 is a transcription factor which upregulates antioxidant genes, producing enzymes to reduce ROS into metabolizable products, such as H_2O_2. Nrf2 is kept inactive in the cytosol by a Keap1–Nrf2 complex. Elevated ROS levels break up this complex, allowing Nrf2 to enter the nucleus and upregulate transcription, a long-term process that occurs over 6–24 h. Therefore, significant elevations in ROS requires a millisecond timescale to effect some cellular damage but a much longer time scale to push the cell into programmed death (if the initial cellular damage does not destroy the cell—necrosis). In the Sridharan model, a network map of Nrf2-related interaction proteins and genetic response elements was constructed as a BN.

The activity of the gene regulatory network was then explored in the context of the Akt pathway (which includes p53 and mdm2) for apoptosis activation. The model included a *Stuck-at-Faults* node state, which means that a particular pathway element's value remains constant regardless of input. This is akin to genetic mutations, whereby a protein remains constitutively ON or OFF, but might also occur in the setting of ROS damage to a protein.

The network was then simulated by adding an *external stress input signal* for 50 time-steps. This was intended to provide an adequately prolonged stimulus to activate apoptosis dynamics. When stress = 0, a network map demonstrated a single point attractor state for the entire network. However, when stress = 1, an attractor cycle (limit cycle) was established, producing activation oscillation.

By comparing multiple simulations over time, a set of fault locations was generated that produced aberrant behavior. The primary input was stress, and the primary output was the Bad/Bcl-2 ratio, where Bad (the Bcl-2-associated death promoter) and Bcl-2, pro- and antiapoptotic factors respectively, are critical in the pathway to apoptosis. Secondary outputs were also defined. Analysis of the network demonstrated the existence of *Homing sequences* as a set of system inputs that bring the network to a particular internal state, regardless of the initial state of genes within the network. Such a Homing sequence was applied to a particular set of initial states and then to the same set but with a fault added to see the effect of such a fault.

It was demonstrated that oxidative stress produced limit cycles where genes proceeded through cycles of upregulation and downregulation based on transcription factor changes. When combined with the Homing sequence algorithm, the network could identify likely fault locations for within the apoptotic network and associate a given fault with its likely outcome.

2.8. Kinetic model with Boolean macroparameters for gating of apoptosis signals

As noted above, Bcl-2 related proteins, including Bad, Bax (Bcl-2-associated X protein), Bak (Bcl-2 homologous antagonist/killer), and others of this family are critical in the process of programmed cell death. In order to extend the BN formalism to provide greater detail, ODEs or stochastic modeling can be used but analyzed in terms of Boolean logic or used in conjunction with BN. Such combined methods have a greater computational load, so generally reduce the scope of the number of interactions that can

be explored. However, they provide greater depth and detail in understanding the dynamics of those pathways that are retained. Unlike BNs, ODE systems can incorporate experimentally determined rate kinetics, such as mRNA degradation rates and binding kinetics for protein–protein interactions.

A recent model by Bogda *et al.* set out to examine levels of control for proapoptotic effector proteins by using a combined ODE and Boolean approach.[16] Activity levels of Bcl-2 family proteins in response to DNA damage (ROS) and external growth factor (GF) signals were modeled in order to determine whether or not these proteins are effective integrators of upstream apoptotic signals transmitted by the Akt and p53 protein pathways. Although these two pathways are somewhat interdependent (i.e., they share common effector molecules), they are independent enough that they can be explored separately. When p53 and Akt are activated ($\{p53,Akt\} = \{1,1\}$), they initiate downstream effectors, resulting in increased accumulation of Bax. High concentration of Bax initiates apoptosis via release of Cytochrome C from mitochondria. Subsequent events involve feedforward and irreversible caspase activation in the common pathway to death.

Major sequences in the two pathways are as follows:

1. Dephosphorylation of the prosurvival Akt pathway leads to apoptosis:
   (a) Dephosphorylated Akt causes dephosphorylation (activation) of Bad; (b) dephosphorylated Bad is released from $Scaffold_{14\text{-}3\text{-}3}$ protein; (c) dephosphorylated Bad initiates Bad–Bcl-x_L binding; (d) Bad–Bcl-x_L binding causes dissociation of Bax–Bcl-x_L, thereby freeing Bax; (e) Bax causes Cytochrome C release; (f) Cytochrome C activates procaspase cleavage; and (g) Caspase cascades lead to apoptosis.
2. Changes in p53 dynamics lead to apoptosis:
   (a) p53 is activated in response to DNA damage (ROS); (b) activated p53 induces synthesis of its own inhibitors; (c) activated p53 also initiates cell cycle arrest and DNA repair; (d) at sufficiently high levels, p53 acts as a transcription factor for Bax and Bak; (e) Bax $\cdots$ —see 1e above.

The model used ODEs to represent species concentrations of relevant proteins and mRNA, including Bax_{mRNA}, Bax, Bcl-x_L, Bad, and Bad-related proteins. Activated procaspases and caspases were also modeled. As in many regulatory networks, bistability plays a critical role in activating and silencing a particular pathway. Bax concentration was identified as a bifurcation parameter: above a threshold concentration of Bax, caspase activation occurs in a feedforward manner and drives the cell irreversibly towards apoptosis. The threshold here was time dependent; that is, when Bax levels were

sufficiently high over a period of time, the switch was activated. This condition was important because short threshold breaches of Bax occur from time to time and in nonapoptotic conditions, and do not normally cause apoptosis. Like other regulated cell decisions, apoptosis involves transcription of new protein. The rate of Bax_{mRNA} formation is modeled as a Hill equation, and is dependent upon activated p53.

The simulations' steady-state responses were analyzed for levels of signal necessary to initiate apoptosis, in the context of a background condition of {p53,Akt} represented by Boolean {0,0}, {1,0}, {0,1}, {1,1}, where 1 represented in each case a proapoptotic state (hence representing unphosphorylated Akt). The consequences of different conditions could then be described as OR or AND gates (OR requiring only activation of one of the two signals, AND requiring both). In these analyses, the Boolean represented initial low or high concentration of the factor; the simulation was then followed, based on its inputs, to determine the consequences once the steady state of the kinetic model was reached. When total levels of Bad were low, only the AND gate pathway led to apoptosis. In this case, both proapoptotic gates {p53,Akt} = {1,1} were required to synergistically activate apoptosis. By contrast, an apoptotic OR gate was found for Bad and Bcl-x_L activation. With high initial concentrations for Bad and Bcl-x_L, all cases except {0,0} generated enough Bax to push the cell towards apoptosis, demonstrating the OR gating. The {0,0} condition led to survival: a situation with low DNA damage and high growth factor. The model also includes the ability to transform an OR gate into an AND gate when Bcl-x_L levels rise, which is a physiologically important aspect of these feedback systems in real cells. Therefore, the relationship between Bax and Bcl-x_L concentrations can effectively determine how the cell responds to proapoptotic or prosurvival signals.

After testing several combinations of parameters and gates, the minimum duration of elevated signals necessary to trigger apoptosis was investigated. Simulation suggested that conditions that required coactivation of both pathways (AND gate), would not settle into an apoptotic state even after 10 h of simulated time. This was a surprising result, considering that Bax and caspase levels were both significantly elevated. After 11 h of simulated time, the system did settle into a state of constitutively high caspase expression, indicative of irreversible apoptosis. Therefore, there is a critical threshold period where proapoptotic and prosurvival signals compete and eventually one wins out over the other—this window would represent an opportunity for targeted therapy. Using the higher inputs which

could lead to apoptosis via the OR gate, the critical duration was much lower, ~3 h.

Macroparameters were defined based on kinetically determined steady-state variables, which describe maximal and minimal concentrations of Bax, and Bax-related protein–protein interaction affinities. The benefit of this approach was to extend the use of Boolean logic by to these other system elements, allowing use of simple inequalities to define these as logic gates as well: for example $(Bax_{tot} + Bad_u > Bcl\text{-}x_L) \rightarrow$ apoptosis. Concentrations of prosurvival and proapoptotic proteins with macroparameters could then be simplified to determine the apoptotic effects of OR or AND gates for these variables. The analysis demonstrated that cells with low levels of free Bcl-x_L will commit to apoptosis via either p53 activation or Akt withdrawal, with little resistance. In contrast, cells with high levels of free Bcl-x_L require increased stimulation by both p53 and Akt to stimulate apoptosis. This model suggests several possible loci of therapeutic intervention, and implies that there is a time dependent, bistable threshold mechanism for pushing the cell towards apoptosis or survival.

2.9. Two-dimensional model of damage and stress response

Degracia *et al.* presented a model of cell damage and response to stress, based on a highly simplified two-dimensional model that lumped the details of molecular mechanisms that were explored in the prior models.[17] Detailed subcellular processes were omitted in order to develop a simplified, top-down understanding of cell fate decisions based on values for damage D and stress response S represented as two coupled ODEs responsive to an injury input I. The linkage between the injury stimulus and change in damage or stress was studied. Damage parameters increased with injury exponentially over time, whereas stress response parameters increased rapidly at first and then gradually declined. When injury was increased slowly from 0, all variables initially rose, leading to saturation of the stress response. However with continued increasing injury, damage is continuously compounded.

Graphically, an injury causes the $\{D,S\}$ point to deviate from the baseline stable attractor at the origin to a new location. The maximum deviation from the origin is described as point $\{D^*,S^*\}$, which is reached at time t_c. After this maximum deviation is reached, injury is dropped to 0 to represent the end of the insult. The state variables will return to $\{0,0\}$, which is interpreted in one of two ways: if $S^* > D^*$, then $\{0,0\}$ represents recovery;

whereas if $D^* > S^*$, $\{0,0\}$ represents cell death. The time it to reach $\{0,0\}$ is the recovery time (t_r) or time to death (t_d). When S^* and D^* were close in magnitude t_r or t_d was increased. This model suggested how the time dependence of recovery from a given magnitude of injury would differ based on the magnitude of competing damage/stress response.

Different response patterns were identified. A characteristic common to all patterns was the existence of a crossover value for injury (termed I_X), representing maximum sustainable injury. This value was dependent both upon the strength of the damage and on the cell's intrinsic strength of response based on the initial state. Cell responses could be classified into four categories, based on the mechanism of stability: (1) Monostable injury course: the manifold had a single attractor that determined cell response. For all I below a threshold value, the cell recovered. Above it, the cell died. (2) Bistable injury courses, type A: A lower and upper attractor were available drawing the system either towards a proapoptotic or prosurvival end result. Unlike the prior case, transition to cell death was abrupt and discontinuous. (3) Bistable injury courses, type B: Bistability was found over an entire range such that cell death could occur at any value of I. In this scenario, high values of S^* can be attained but only over a long period of time (high t_d). (4) Double bistable injury courses combine both types of bistability with a combined model. Due to bistability at the origin, a small injury can cause cell death.

These models can be used to help explain delayed death after injury, as t_d and t_r lengthen in situations where D^* is only slightly greater than S^*. During recovery from an injury, there is a point at which the damage has subsided, but the stress response remains elevated, due to the different time courses for these processes. This can be used to predict the effects of an ischemic preconditioning. By contrast, a situation in which the initial conditions involve preexisting damage can allow cell death even with small injury, as in the case with prior damage due to hypertension or diabetes mellitus. These results also suggest explanations for some of the difficulties involved in clinical translation due to the heterogeneity of the clinical conditions compared to the homogeneous $\{D^*,S^*\}$ utilized in animal experimentation.

2.10. Analyzing cell fate decisions with an ODE-based regulatory gene network model

Rapidly after ischemic insult, direct metabolic effects and changes in membrane potential dominate. After longer times, protein cascades take effect. Still later, for those cells that still survive, additional genetic factors kick

in to further transform the cell through substantial new transcription and translation.

A model for cellular-level genetic factors involved in stroke was formulated by McDermott *et al.*[18] to assess how gene expression changes over time in response to stroke. A network of expressed proteins was defined as a set of gene modules (termed a cluster), each with a similar function. Information about how these modules interact was gleaned from a high-throughput analysis of transcription information from mouse stroke models, using mice that had been given a preconditioning stimulus of lipopolysaccharides, CpG-oligonucleotides, brief mild ischemia, saline (control), or sham surgery (control). Model parameters were defined based on levels of gene expression across many cells over time from 3 to 72 h after infarct. Probe sets were used to identify intensity of response in the various clusters (Fig. 11.2).

Cluster analyses were then used to determine hierarchical relationships. Inferred causative relationships were used to generate ODE models of steady-state behavior using an inference algorithm. The gene clusters with the highest downstream upregulation of effector proteins were used to generate an optimized network. Downstream expression of genes was modeled by changing regulatory inputs to look at differences in mean cluster expression over time. The observed results were then compared to results predicted from the optimal network, and against a consensus prediction from other nonoptimized network models.

A major result of the paper was identification of which gene clusters were upregulated by particular preconditioning stimuli. Mild ischemia strongly altered genes in cluster 5, which contains regulatory genes for metabolic processes and metabolic regulation. This suggested that cluster 5 might play a major role in neuroprotection following transient, mild ischemic insults. All of the preconditioning paradigms upregulated apoptosis and inflammatory gene clusters, and all led to significantly greater levels of protection compared to control. A neuroprotective gene for TNF-α was found in the inflammatory cluster, suggesting that mice deficient in this gene would lose some of the benefits of preconditioning.

2.11. Modeling evolution of the penumbra

Although the focus of this chapter is on cellular and subcellular pathways implicated in ischemia, these changes occur at the same time in different proportions in different cells depending on the location of a particular cell within the umbra or penumbra of a stroke. Effects at the single cell level are

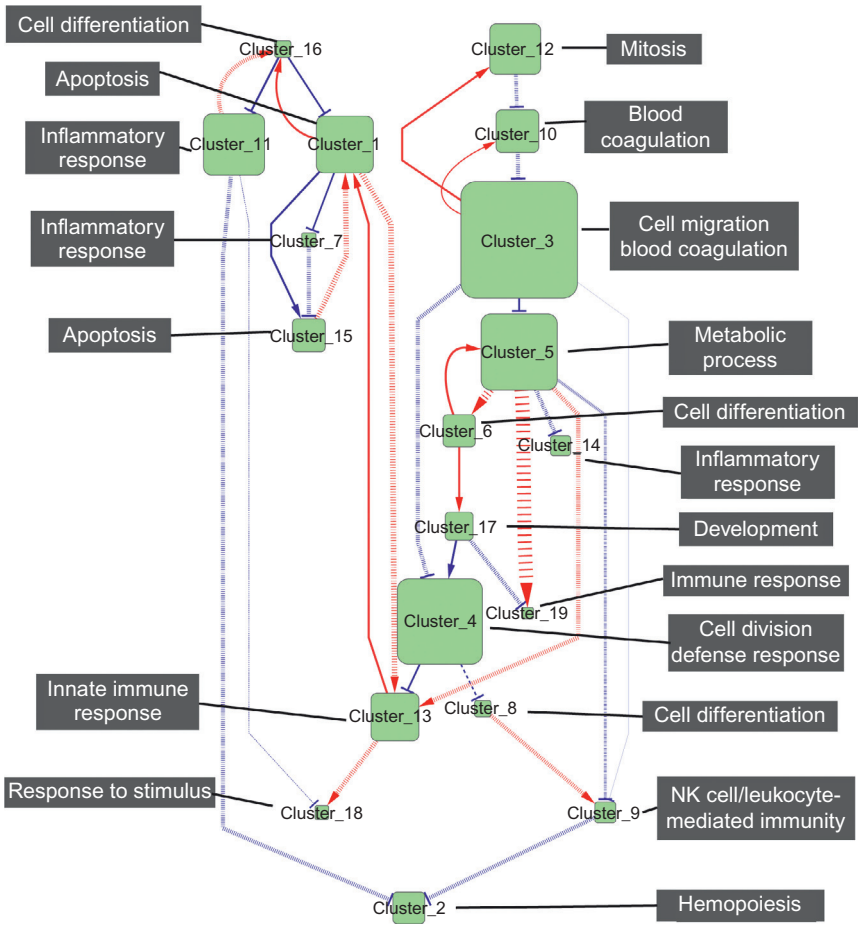

Figure 11.2 Multiple gene clusters involved in response to stroke. *Taken from fig. 8 of Ref. 18.*

also compounded at the higher scale, as toxic agents and ion shifts are spread between cells across the tissue. Ultimately, all damaging results of ischemia stem from loss of substrates for energy production. Nutrient delivery at the level of blood and of extracellular tissue is therefore highly relevant in creating the microenvironment within which the cell's molecular processes take place. Regional variation is an important feature in the brain as compared to other organs; variations in vascular patterns are common and the severity of ischemic damage can vary significantly based on whether or not a region has enough anastomotic connections to neighboring blood

supplies. The affected stroke tissue is usually defined by examining regional differences in blood delivery. Assessing levels of nutrient flow is also clinically important in defining the severity of stroke. A variety of other factors, both environmental and genetic, can also contribute to morphological and molecular differences in the extent of penumbral regions.[14] Common to all penumbrae are characteristic edematous and inflammatory changes.

An early computational model linking molecular changes in the penumbral tissue with cerebral blood flow was published by Revett *et al.* in 1998.[19] This model focused on generation of the penumbra, at tissue scale, but incorporated cell-level modeling of basic metabolic processes. The model simulated depolarizations found in ischemic tissue that produce waves of pathological activation across the tissue, termed cortical spreading depression. In this model, cortex is represented as a hexagonal array of elements, each of which represents a single cell and contains variables for intracellular and extracellular ionic concentrations, levels of blood flow, and levels of metabolites. General impairment and intactness indices reflect levels of intact function of a given variable and of malfunction of the same variable, respectively. Extracellular diffusive K^+ was also simulated. Importantly, this model included discrete spatial zones. Varying parameters allowed exploration of effects such as relative damage depending on the ratio of core infarct to penumbra. The Revett model also predicted the relationship between cortical spreading depression and infarct size, and the balance between control of energy metabolism versus delivery of metabolites.

Duval *et al.* modeled cellular consequences of changes in cerebral blood flow.[20] Like Revett *et al.*, the authors model regions of brain tissue as a set of adjacent zones. Vascular regions are defined for specific zones. This method also allowed simulation of cellular regions with overlapping vasculature, an important factor in the brain's ischemic response. The Duval model used four primary parameters: cerebral blood flow, rate of oxygen extraction from blood, metabolic rate of oxygen use by tissue, and the apparent diffusion coefficient of water. A *survival delay variable* was also used to quantify the decay of tissue in the penumbra from functional, to salvageable, to necrotic. Results of running the model many times with varying initial conditions yielded information about patterns of morphological changes in penumbral regions. Severely ischemic penumbra tissue had altered cellular metabolism, and generally was not salvageable, whereas the edematous penumbra tissue appeared to retain greater recovery potential. This model clarified ways in which extracellular nutrient parameters might affect the generation of penumbral regions, and what types of edematous tissue might be salvageable.

The core of all ischemic infarcts becomes necrotic rapidly. It has been well documented that this necrotic core experiences changes different from the slower apoptotic and necrotic death that occurs in the surrounding tissue.[14] Necrotic cells initiate a series of local events, which will lead to cytotoxic edematous changes as noted in the prior section.

The model by Di Russo *et al.* was used to evaluate the contribution of inflammatory processes to the further development of edema in the penumbra.[22] The model uses proportional densities of healthy, dying, and dead cells, as well as leukocytic cells, to evaluate the diffusive effects of inflammatory chemokines and cytokines that react with local cells to modify the ischemic insult. Partial differential equations are used to describe how these molecular factors alter the densities of dead, dying and healthy cells over time. The change in necrotic tissue was considered to be the difference between the proportion of healthy cells that are dying and the proportion of necrotic cells that are being phagocytized at a given time-step. Results showed that the initial ratio of dying cell types (necrotic vs. apoptotic) was critical in determining brain response to inflammatory events, with a higher percentage of initial necrotic cells, causing a larger inflammatory response, which then augmented apoptosis in the surrounding region. Depending on the size of the infarct, the inflammatory response could have either negative or neuroprotective effects, related to the concept of ischemic preconditioning.

3. PITFALLS AND OUTLOOK

The most basic problem in all of these models is the necessity for omission of many biological parameters either because they are not known or because their inclusion makes the model unmanageable. Simplification is always a necessity in modeling but gives the risk of leaving out some critical factors. For example, none of the models include the more than 20 different channels and pumps that play a role in ionic fluctuation across the membrane, including some that have not yet been fully defined experimentally. In the case of intracellular organelles, the ER and mitochondria, there are still no experimental methods that allow activity across these internal membranes to be fully explored.

Some of the formalisms themselves necessarily limit the degree of verisimilitude. Clearly the BN formalism oversimplifies the relationships between state variables by defining them in terms of binary state switching without kinetics. BN modeling also does not account for transition states for

variables, which may be important in ischemic pathways. However the reductionism of BN models is useful for exploration of large cascade models, in which many simulations are run to determine system dynamics.

Along similar lines, it has been noted in this chapter that ischemia is a multicellular, complex network phenomenon. Breaking the pathway components into chunks that can be adequately modeled is a necessary step given our current abilities in computing and our understanding of how these pathways interact. However, such a divisive and reductive approach may limit the usefulness of models of a system that is inherently multiscale, where the whole is greater than the sum of its parts due to emergent phenomenology. It has, in fact, been argued that the strength of modeling lies in the possibility of exploration across scales. Such cross-scale investigation is often difficult to do experimentally, where different techniques are required for explorations at different scales, different techniques that often are difficult or impossible to use in combination.

Another major difficulty, common to nearly all models of ischemia, is setting of parameters and initial values. Parameters are often be taken from models of healthy tissue and may be different than those found in ischemic tissue, where proteins are present in different phosphorylation states. Additionally, these models are typically chimeric with parameters gathered from different cell types from different species, at different animal ages. For example, the Magnus and Keizer model of ATP and Ca^{++} regulation, widely adopted for use in ischemia models, was based on pancreatic beta cells. It is now appreciated that cells vary enormously in their proteomic expression, genetic regulation, and intercellular communication, based on species type, tissue type, and even location within a seemingly homogeneous tissue.

Many of the models presented in this chapter do not deal at all with the spatial aspects of intracellular communication, making the assumption of a *well-mixed* solution so as to work with reactions without diffusion. However neurons and glia are among the most morphologically diverse and highly compartmentalized cells in the body: there are major differences between molecular machinery in spines, dendrites, soma, and axon. Full reaction–diffusion modeling of these factors is still rudimentary, made more difficult by the fact that different simulation techniques will need to be used for these different compartments. An additional factor that can still not be incorporated into models is changes in cell morphology due to plasticity or damage.

Computer modeling of ischemia can expand our understanding of the cellular and subcellular processes involved in ischemia, particularly in defining the ionic fluctuations of cytotoxicity, gene regulation and transcription,

and cell fate decisions of cells under metabolic stress. Many questions still remain. What are the mechanisms by which cells switch between recovery and death in response to stressful stimuli? How do inflammatory factors affect apoptotic signaling in the penumbra? What is the role of cell-to-cell signaling in modulating the tissue response to ischemia? What genetic and environmental factors can predispose a patient to, or protect a patient from, ischemic damage? Several approaches to modeling have been used to tackle various aspects of ischemic pathways. A major challenge for the future will be figuring out how to effectively integrate these approaches to create multiscale models of ischemia incorporating information from the molecular to brain levels.

REFERENCES

1. *Center for Disease Control*, Leading causes of death, CDC fact sheet; 2011.
2. Saftenku EE, Friel DD. Chapter 26: combined computational and experimental approaches to understanding the CA^{2+} regulatory network in neurons. In: Islam S, ed. *Calcium Signaling*. New York, NY: Springer; 2012 Advances in Experimental Medicine and Biology. Vol. 740.
3. Bartus RT. The calpain hypothesis of neurodegeneration: evidence for a common cytotoxic pathway. *Neuroscientist*. 1997;3(5):314–327.
4. Dronne M-A, Boissel J-P, Grenier E. A mathematical model of ion movements in grey matter during a stroke. *J Theor Biol*. 2006;240(4):599–615.
5. Bartol Jr TM, Land BR, Salpeter EE, Salpeter MM. Monte carlo simulation of miniature endplate current generation in the vertebrate neuromuscular junction. *Biophys J*. 1991;59:1290–1307.
6. Dronne M-A, Boissel J-P, Grenier E, et al. Mathematical modelling of an ischemic stroke: an integrative approach. *Acta Biotheor*. 2004;52(4):255–272.
7. Verheul HB, Balazs R, Berkelbach van der Sprenkel JW, et al. Comparison of diffusion-weighted MRI with changes in cell volume in a rat model of brain injury. *NMR Biomed*. 1994;7(1–2):96–100.
8. Diekman CO, Fall CP, Lechleiter JD, Terman D. Modeling the neuroprotective role of enhanced astrocyte mitochondrial metabolism during stroke. *Biophys J*. 2013;104(8):1752–1763.
9. Magnus G, Keizer J. Model of beta-cell mitochondrial calcium handling and electrical activity. I. Cytoplasmic variables. *Am J physiol*. 1998;274(4 Pt 1):C1158–C1173.
10. Oster AM, Thomas B, Terman D, Fall CP. The low conductance mitochondrial permeability transition pore confers excitability and CICR wave propagation in a computational model. *J Theor Biol*. 2011;273(1):216–231.
11. Magnus G, Keizer J. Minimal model of beta-cell mitochondrial Ca^{2+} handling. *Am J Physiol*. 1997;273(2 Pt 1):C717–C733.
12. Heuett WJ, Periwal V. Autoregulation of free radicals via uncoupling protein control in pancreatic beta-cell mitochondria. *Biophys J*. 2010;98(2):207–217.
13. Alam MJ, Devi GR, Ravins, Ishrat R, Agarwal SM, Brojen Singh RK. Switching p53 states by calcium: dynamics and interaction of stress systems. *Mol BioSyst*. 2013;9(3):508–521.
14. Lipton P. Ischemic cell death in brain neurons. *Physiol Rev*. 1999;79(4):1431–1568.

15. Mai Z, Liu H. Boolean network-based analysis of the apoptosis network: irreversible apoptosis and stable surviving. *J Theor Biol*. 2009;259(4):760–769.
16. Bogda MN, Hat B, Kocha Czyk M, Lipniacki T. Levels of pro-apoptotic regulator Bad and anti-apoptotic regulator Bcl-xL determine the type of the apoptotic logic gate. *BMC Syst Biol*. 2013;7(1):67.
17. DeGracia DJ, Huang ZF, Huang S. A nonlinear dynamical theory of cell injury. *J Cereb Blood Flow Metab*. 2012;32(6):1000–1013.
18. McDermott JE, Jarman K, Taylor R, et al. Modeling dynamic regulatory processes in stroke. *PLoS Comput Biol*. 2012;8(10):e1002722.
19. Revett K, Ruppin E, Goodall S, Reggia JA. Spreading depression in focal ischemia: a computational study. *J Cereb Blood Flow Metab*. 1998;18(9):998–1007.
20. Duval V, Chabaud S, Girard P, Cucherat M, Hommel M, Boissel JP. Physiologically based model of acute ischemic stroke. *J Cereb Blood Flow Metab*. 2002;22(8):1010–1018.
21. Sridharan S, Layek R, Datta A, Venkatraj J. Boolean modeling and fault diagnosis in oxidative stress response. *BMC Genomics*. 2012;13(Suppl 6):S4.
22. Di Russo C, Lagaert J-B, Chapuisat G, Dronne M-A. A mathematical model of inflammation during ischemic stroke. In: *ESAIM: Proceedings*; 2010:15–33. EDP Sciences; Vol. 30.